Biomedical Optics EXPRESS

Improved two-photon imaging of living neurons in brain tissue through temporal gating

Vini Gautam,[1] Jack Drury,[1] Julian M. C. Choy,[1] Christian Stricker,[1,2] Hans-A. Bachor,[3] and Vincent R. Daria[1,*]

[1]*John Curtin School of Medical Research, The Australian National University, Canberra, ACT 2601, Australia*
[2]*Medical School, The Australian National University, Canberra, ACT 2601, Australia*
[3]*Research School of Physics and Engineering, The Australian National University, Canberra, ACT 2601, Australia*
[*]*vincent.daria@anu.edu.au*

Abstract: We optimize two-photon imaging of living neurons in brain tissue by temporally gating an incident laser to reduce the photon flux while optimizing the maximum fluorescence signal from the acquired images. Temporal gating produces a bunch of ~10 femtosecond pulses and the fluorescence signal is improved by increasing the bunch-pulse energy. Gating is achieved using an acousto-optic modulator with a variable gating frequency determined as integral multiples of the imaging sampling frequency. We hypothesize that reducing the photon flux minimizes the photo-damage to the cells. Our results, however, show that despite producing a high fluorescence signal, cell viability is compromised when the gating and sampling frequencies are equal (or effectively one bunch-pulse per pixel). We found an optimum gating frequency range that maintains the viability of the cells while preserving a pre-set fluorescence signal of the acquired two-photon images. The neurons are imaged while under whole-cell patch, and the cell viability is monitored as a change in the membrane's input resistance.

OCIS codes: (170.3880) Medical and biological imaging; (170.3660) Light propagation in tissues; (140.0140) Lasers and laser optics; (170.2520) Fluorescence microscopy; (170.6930) Tissue; (110.0110) Imaging systems.

References and links

1. W. Denk, J. H. Strickler, and W. W. Webb, "Two-photon laser scanning fluorescence microscopy," Science **248**(4951), 73–76 (1990).
2. F. Helmchen and W. Denk, "Deep tissue two-photon microscopy," Nat. Methods **2**(12), 932–940 (2005).
3. T. Abraham, J. A. Hirota, S. Wadsworth, and D. A. Knight, "Minimally invasive multiphoton and harmonic generation imaging of extracellular matrix structures in lung airway and related diseases," Pulm. Pharmacol. Ther. **24**(5), 487–496 (2011).
4. I. A. Ghouri, A. Kelly, F. L. Burton, G. L. Smith, and O. J. Kemi, "2-photon excitation fluorescence microscopy enables deeper high-resolution imaging of voltage and Ca^{2+} in intact mice, rat, and rabbit hearts," J. Biophotonics **8**(1-2), 112–123 (2015).
5. R. J. Low, Y. Gu, and D. W. Tank, "Cellular resolution optical access to brain regions in fissures: imaging medial prefrontal cortex and grid cells in entorhinal cortex," Proc. Natl. Acad. Sci. U.S.A. **111**(52), 18739–18744 (2014).
6. N. R. Wilson, J. Schummers, C. A. Runyan, S. X. Yan, R. E. Chen, Y. Deng, and M. Sur, "Two-way communication with neural networks in vivo using focused light," Nat. Protoc. **8**(6), 1184–1203 (2013).
7. K. Svoboda and R. Yasuda, "Principles of two-photon excitation microscopy and its applications to neuroscience," Neuron **50**(6), 823–839 (2006).
8. V. Nikolenko, K. E. Poskanzer, and R. Yuste, "Two-photon photostimulation and imaging of neural circuits," Nat. Methods **4**(11), 943–950 (2007).
9. A. M. Packer, L. E. Russell, H. W. P. Dalgleish, and M. Häusser, "Simultaneous all-optical manipulation and recording of neural circuit activity with cellular resolution *in vivo*," Nat. Methods **12**(2), 140–146 (2014).
10. M. A. Go, M. S. To, C. Stricker, S. Redman, H.-A. Bachor, G. J. Stuart, and V. R. Daria, "Four-dimensional multi-site photolysis of caged neurotransmitters," Front. Cell. Neurosci. **7**, 231 (2013).

#247308 Received 6 Aug 2015; revised 11 Sep 2015; accepted 11 Sep 2015; published 17 Sep 2015

11. M. A. Go, C. Stricker, S. Redman, H.-A. Bachor, and V. R. Daria, "Simultaneous multi-site two-photon photostimulation in three dimensions," J. Biophotonics **5**(10), 745–753 (2012).
12. B. E. Losavio, V. Iyer, and P. Saggau, "Two-photon microscope for multisite microphotolysis of caged neurotransmitters in acute brain slices," J. Biomed. Opt. **14**(6), 064033 (2009).
13. D. J. Wallace, S. Meyer zum Alten Borgloh, S. Astori, Y. Yang, M. Bausen, S. Kügler, A. E. Palmer, R. Y. Tsien, R. Sprengel, J. N. Kerr, W. Denk, and M. T. Hasan, "Single-spike detection in vitro and in vivo with a genetic Ca^{2+} sensor," Nat. Methods **5**(9), 797–804 (2008).
14. H. Lütcke, M. Murayama, T. Hahn, D. J. Margolis, S. Astori, S. M. Zum Alten Borgloh, W. Göbel, Y. Yang, W. Tang, S. Kügler, R. Sprengel, T. Nagai, A. Miyawaki, M. E. Larkum, F. Helmchen, and M. T. Hasan, "Optical recording of neuronal activity with a genetically-encoded calcium indicator in anesthetized and freely moving mice," Front. Neural Circuits **4**, 9 (2010).
15. C. Stosiek, O. Garaschuk, K. Holthoff, and A. Konnerth, "In vivo two-photon calcium imaging of neuronal networks," Proc. Natl. Acad. Sci. U.S.A. **100**(12), 7319–7324 (2003).
16. N. Olivier, A. Mermillod-Blondin, C. B. Arnold, and E. Beaurepaire, "Two-photon microscopy with simultaneous standard and extended depth of field using a tunable acoustic gradient-index lens," Opt. Lett. **34**(11), 1684–1686 (2009).
17. P. A. Kirkby, K. M. Srinivas Nadella, and R. A. Silver, "A compact Acousto-Optic Lens for 2D and 3D femtosecond based 2-photon microscopy," Opt. Express **18**(13), 13720–13745 (2010).
18. G. Thériault, M. Cottet, A. Castonguay, N. McCarthy, and Y. De Koninck, "Extended two-photon microscopy in live samples with Bessel beams: steadier focus, faster volume scans, and simpler stereoscopic imaging," Front. Cell. Neurosci. **8**, 139 (2014).
19. P. Lai, L. Wang, J. W. Tay, and L. V. Wang, "Photoacoustically guided wavefront shaping for enhanced optical focusing in scattering media," Nat. Photonics **9**(2), 126–132 (2015).
20. A. P. Mosk, A. Lagendijk, G. Lerosey, and M. Fink, "Controlling waves in space and time for imaging and focusing in complex media," Nat. Photonics **6**(5), 283–292 (2012).
21. U. K. Tirlapur, K. König, C. Peuckert, R. Krieg, and K.-J. Halbhuber, "Femtosecond near-infrared laser pulses elicit generation of reactive oxygen species in mammalian cells leading to apoptosis-like death," Exp. Cell Res. **263**(1), 88–97 (2001).
22. H. He, K. T. Chan, S. K. Kong, and R. K. Y. Lee, "Mechanism of oxidative stress generation in cells by localized near-infrared femtosecond laser excitation," Appl. Phys. Lett. **95**(23), 233702 (2009).
23. S. W. Botchway, P. Reynolds, A. W. Parker, and P. O'Neill, "Use of near infrared femtosecond lasers as sub-micron radiation microbeam for cell DNA damage and repair studies," Mutat. Res. **704**(1-3), 38–44 (2010).
24. A. Hopt and E. Neher, "Highly nonlinear photodamage in two-photon fluorescence microscopy," Biophys. J. **80**(4), 2029–2036 (2001).
25. K. König, P. T. C. So, W. W. Mantulin, and E. Gratton, "Cellular response to near-infrared femtosecond laser pulses in two-photon microscopes," Opt. Lett. **22**(2), 135–136 (1997).
26. X. Chen, U. Leischner, Z. Varga, H. Jia, D. Deca, N. L. Rochefort, and A. Konnerth, "LOTOS-based two-photon calcium imaging of dendritic spines in vivo," Nat. Protoc. **7**(10), 1818–1829 (2012).
27. V. Magidson and A. Khodjakov, "Circumventing photodamage in live-cell microscopy", in *Methods in Cell Biology*, S. Greenfield and E. W. David eds. (Vol. 114, 2013).
28. N. Ji, J. C. Magee, and E. Betzig, "High-speed, low-photodamage nonlinear imaging using passive pulse splitters," Nat. Methods **5**(2), 197–202 (2008).
29. S. Tang, T. B. Krasieva, Z. Chen, G. Tempea, and B. J. Tromberg, "Effect of pulse duration on two-photon excited fluorescence and second harmonic generation in nonlinear optical microscopy," J. Biomed. Opt. **11**(2), 020501 (2006).
30. E. Beaurepaire, M. Oheim, and J. Mertz, "Ultra-deep two-photon fluorescence excitation in turbid media," Opt. Commun. **188**(1-4), 25–29 (2001).
31. G. Donnert, C. Eggeling, and S. W. Hell, "Major signal increase in fluorescence microscopy through dark-state relaxation," Nat. Methods **4**(1), 81–86 (2007).
32. G. Donnert, C. Eggeling, and S. W. Hell, "Triplet-relaxation microscopy with bunched pulsed excitation," Photochem. Photobiol. Sci. **8**(4), 481–485 (2009).
33. G. McConnell and E. Riis, "Two-photon laser scanning fluorescence microscopy using photonic crystal fiber," J. Biomed. Opt. **9**(5), 922–927 (2004).
34. C. Xu and W. W. Webb, "Measurement of two-photon excitation cross sections of molecular fluorophores with data from 690 to 1050 nm," J. Opt. Soc. Am. B **13**(3), 481–491 (1996).
35. D. Kobat, N. G. Horton, and C. Xu, "In vivo two-photon microscopy to 1.6-mm depth in mouse cortex," J. Biomed. Opt. **16**(10), 106014 (2011).
36. K. Fujita, M. Kobayashi, S. Kawano, M. Yamanaka, and S. Kawata, "High-resolution confocal microscopy by saturated excitation of fluorescence," Phys. Rev. Lett. **99**(22), 228105 (2007).
37. E. Ronzitti, B. Harke, and A. Diaspro, "Frequency dependent detection in a STED microscope using modulated excitation light," Opt. Express **21**(1), 210–219 (2013).
38. M. Yamanaka, K. Saito, N. I. Smith, S. Kawata, T. Nagai, and K. Fujita, "Saturated excitation of fluorescent proteins for subdiffraction-limited imaging of living cells in three dimensions," Interface Focus **3**(5), 20130007 (2013).

#247308 Received 6 Aug 2015; revised 11 Sep 2015; accepted 11 Sep 2015; published 17 Sep 2015

1. Introduction

Two-photon (2P) microscopy is extensively used for imaging optically thick biological tissues because of its deeper penetration and intrinsic three-dimensional resolution [1,2]. Applications include high resolution imaging of structures, as well as functional dynamics of physiological systems such as the brain, heart and lungs [3–6]. In neuroscience, 2P microscopes have been utilized for manipulation of neuronal activity, as well as for imaging neuronal activity using fluorescent indicators, both *in vitro* and *in vivo* [7–9]. With this technique, non-invasive photochemical stimulation of neurons can be achieved using methods such as photolysis of caged neurotransmitters, [10–12] and neuronal function can be monitored by imaging fluorescence from various reports of neuronal activity (*e.g.* Ca^{2+} indicators and voltage-sensitive dyes) [13–15].

Optimizing and re-designing 2P microscopes to suit particular applications have been implemented [16–20]. Optimizations in terms of speed of image acquisition as well as improved imaging through thick biological tissues are primary concerns. However, when used for imaging living cells, extra precautions are required to maintain the viability of cells. The diffraction-limited spot size in sub-micrometer region with mW orders of average power of the near infrared (NIR) laser can result in energy flux of the order of 10^{12} Wcm^{-2} and photon flux close to 10^{32} photons cm^{-2} s^{-1}. For live biological samples, such high photon flux results in a delivery of extremely high power to the cell or tissue components thereby affecting cell vitality and could cause irreversible photodamage. Previous studies on various cell types have established that the mechanism of photodamage to cells during 2P imaging is biochemical in nature. Photodamage is caused by the generation of destructive oxygen radicals and singlet oxygen upon incident NIR femtosecond laser pulses, which result in oxidative stress, indirect DNA damage and cell apoptosis [21–23]. In some studies, 2P excitation has been shown to directly hamper cell division, as well as cause lysis and disintegration of the cell membrane resulting in their death [24,25]. Although there have been many studies that have focused on the detection and quantification of photodamage to cells during 2P imaging, there have been few reports that have addressed overcoming this issue [26–28].

Utilizing the 2P technique for imaging live biological samples also requires obtaining high fluorescence yield with reduced photobleaching of fluorophores. The biochemical processes in the cells together with the photochemical properties of the fluorophores result in photobleaching and reduced fluorescence signal during imaging. Strategies to achieve higher fluorescence and lesser photobleaching have focused on reducing the light-excitation dose and simultaneously maintaining a high fluorescence signal. This has been achieved by varying average and peak power, pixel dwell-time, repetition rate and pulse duration of the incident imaging laser pulses [29–33]. For instance, it has been shown that reducing the laser pulse width to sub - 100 femtosecond enhances the two-photon-excited fluorescence from the sample and enables imaging of deeper layers of biological samples [29,33]. Reducing the repetition rate of femtosecond pulses to < 200 kHz (regenerative amplification) has also been utilized for higher fluorescence emission and deeper penetration depth [30]. Also, temporal gating of the femtosecond laser pulses in the range of 0.5-40 MHz have been shown to correspond to the triplet state relaxation of common fluorophores, and hence has been proposed as the optimum gating range for signal gain in fluorescence microscopy [31,32]. While these studies focus on achieving reduced photobleaching and enhanced fluorescence from common dyes; they have not highlighted or addressed the issue of light-induced alteration of the cell membrane.

In this work, we show that reduction of the photon flux while obtaining enhanced fluorescence emission from the sample could preserve the viability of living neurons in brain tissue. We reduce the incident photon flux by temporally gating the laser thereby producing a periodic bunch of femtosecond pulses. Temporal gating of the incident laser is achieved via an acousto-optic modulator (AOM) with frequency chosen as integral multiples of the

#247308 Received 6 Aug 2015; revised 11 Sep 2015; accepted 11 Sep 2015; published 17 Sep 2015

imaging sampling frequency. The gating produces a bunch of ~10 femtosecond pulses and is synchronized with the imaging sampling rate, with a setting of one to six bunches per pixel. Temporal gating reduces the average power delivered onto the sample. To improve the fluorescence yield, we compensate by increasing the bunch-pulse energy. However, high bunch-pulse energy compromises cell viability as it increases the probability of photodamage to the neuron. Here, we show that there is an optimum gating frequency range that produces enhanced fluorescence signal but with minimal effect on the cell membrane and therefore maintaining cell viability.

2. Methods

2.1 Optical setup

The custom-built 2P microscope used in the experiments is part of system described in our previous works [10,11]. Figure 1(a) describes the basic geometry of the system. For 2P fluorescence imaging, galvanometer (GM) scanning mirrors were used to scan a linearly polarized TEM_{00} laser beam from a NIR Ti:S laser (Coherent Inc. MIRA 900) pumped by a 12W optically pumped semiconductor laser (Coherent Verdi G). The same sample region was viewed via an upright differential interference contrast (DIC) microscope (Olympus BX50WI) for patching the neuron with a microelectrode. DM1 reflects the NIR laser beam (<810 nm wavelength) to the objective and transmits NIR light (>810 nm) from the light source at the bottom of the microscope for DIC imaging mode. A 2P image is obtained by raster scanning the laser along the sample using galvanometer mirrors (GM) and relay lenses (L). The fluorescence from the sample is directed to a second dichroic mirror (DM2), which reflects wavelengths below 700 nm onto a photomultiplier tube (PMT). The imaging routine is controlled using custom software developed in *Labview* (National Instruments), with intensity control using a polarizing beam splitter (PBS) and a half-wave (λ/2) plate on a motorized rotating stage.

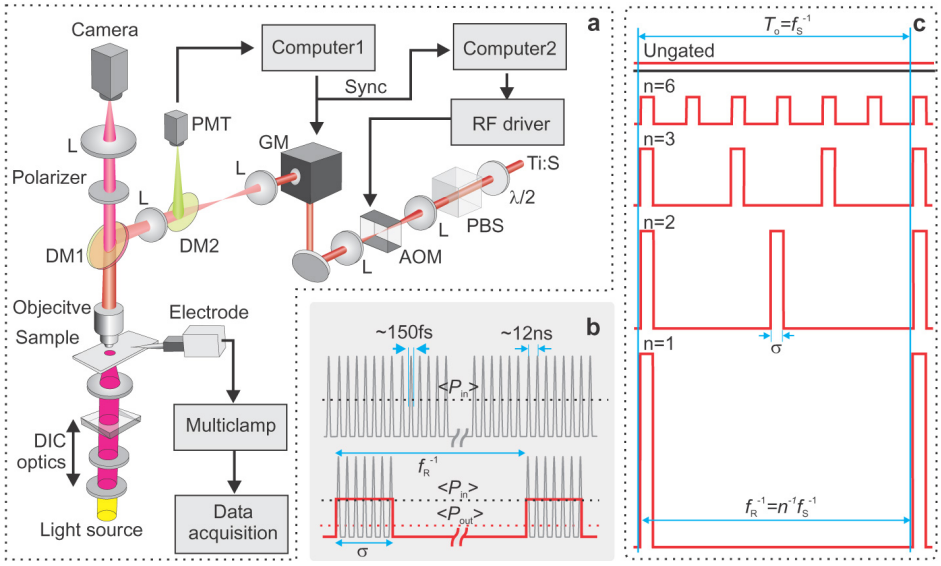

Fig. 1. (a) Schematic showing the experimental set-up with temporal gating using an acousto-optic modulator (AOM). (b) Schematic showing a bunch of femtosecond pulses gated with a bunch pulse width, σ~140ns, period of $1/f_R$ (where f_R is the gating frequency) and average power $\langle P_{in} \rangle$ before and $\langle P_{out} \rangle$ after the AOM. The top trace depicts the un-gated femtosecond laser. Bottom trace shows temporal gating where $\langle P_{our} \rangle$ is less than $\langle P_{in} \rangle$. (c) Schematic depicting a constant energy in one pixel (pixel dwell time T_o = 2.5 μs) with varying gating frequencies. Note that a low f_R requires a high $\langle P_{in} \rangle$. Here f_s is the sampling frequency and $n = f_R/f_s$ is the number of bunches per pixel.

#247308 Received 6 Aug 2015; revised 11 Sep 2015; accepted 11 Sep 2015; published 17 Sep 2015

Temporal gating was achieved using an AOM (AA Opto ST110-A1-B4) along the laser path prior to the 2P microscope. The AOM was driven by a radio-frequency driver (AA Opto MODA110-B4-33). Timing and triggering of the AOM driver is achieved with a digital output signal from a data acquisition interface (National Instruments PCIe-6363) where a *Labview* program sets the gating frequency synchronized with the image sampling routine. Although the entire imaging and gating routine can be controlled using a single computer, the current setup uses separate controls where Computer 1 is used for imaging while Computer 2 is used to drive the gating routine. The average laser powers, $\langle P_{in} \rangle$ and $\langle P_{out} \rangle$ were monitored before and after the AOM, respectively. $\langle P_{out} \rangle$ is effectively measured at the sample plane. Intuitively, temporal gating reduces the average power delivered onto the sample (Fig. 1(b)). We then compensate the bunch-energy by increasing $\langle P_{in} \rangle$ while keeping a fixed bunch width, σ (Fig. 1(c)).

2.2 Calibration

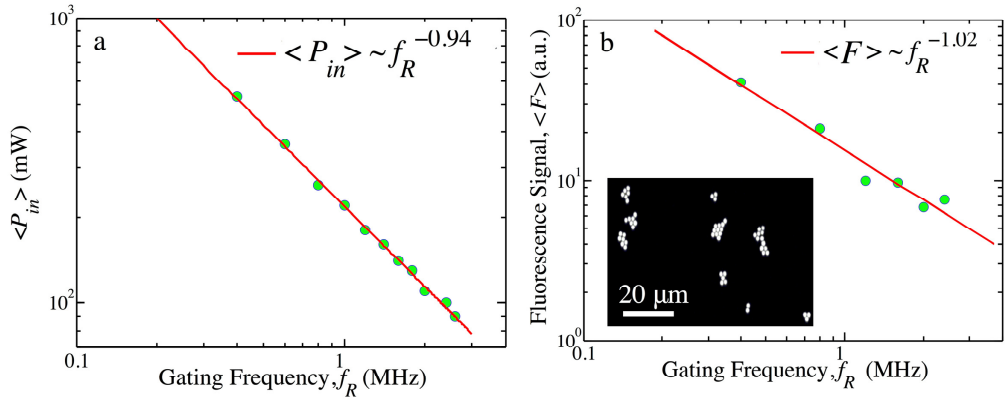

Fig. 2. (a) Relation between gating frequency, f_R and $\langle P_{in} \rangle$ for a constant $\langle P_{out} \rangle$ = 0.5 mW, shown on a log-log plot. The data fit has a slope of −0.94. (b) Relation between gating frequency, f_R and fluorescence, F for a constant $\langle P_{out} \rangle$ = 1 mW, shown on a log-log plot. The data fit has a slope of −1.02. Inset shows an image of the fluorescent microspheres used to perform these experiments.

From the conservation of energy, maintaining a constant $\langle P_{out} \rangle$ sets $\langle P_{in} \rangle$ to follow an inverse relation with gating frequency given by

$$< P_{out} > f_R^{-1} =< P_{in} > \sigma \tag{1}$$

where σ is the bunch width, and f_R is the gating frequency. Such inverse relation is also shown in Fig. 2(a). We then analyzed how temporal gating affects the fluorescence signal for rendering an image. Incorporating the standard 2P relation [34], the time-integrated fluorescence signal per pixel $\langle F \rangle$ measured within a finite pixel dwell time, $T_o = f_s^{-1}$ (where f_s is the sampling frequency) is given by

$$< F > \approx n < P_{in}^2 > \tag{2}$$

where $n = T_o f_R$ is the number of bunches within T_o. Combining Eqs. (1) and (2), we obtain the following relation:

$$< F > \approx \frac{T_o < P_{out}^2 >}{\sigma^2} \frac{1}{f_R} \tag{3}$$

#247308 Received 6 Aug 2015; revised 11 Sep 2015; accepted 11 Sep 2015; published 17 Sep 2015

We evaluated Eq. (3) by imaging 2 μm diameter fluorescent latex microspheres (Molecular Probes, Inc) with temporal gating set-up while maintaining a constant $<P_{out}>$ = 1 mW. The microspheres emit green fluorescence following the 2P excitation from a focused near-infrared femtosecond pulsed laser. The fluorescence intensity from the microspheres was quantified using *ImageJ* (National Institutes of Health) by subtracting the background from the maximum fluorescence signal of a group of microspheres. Our results show that for the same $<P_{out}>$, the fluorescence intensity increases at lower gating frequencies (Fig. 2(b)), and Eq. (3) fits well with the experimental data.

2.3 Preparation of brain slices

Parasagittal brain slices (300 μm) were obtained from 15 to 19-day-old Wistar rats. Upon following standard procedures for isolating the brain from the animal, the slices were cut with a vibratome (Leica VT1200S) in ice-cold oxygenated artificial cerebrospinal fluid (ACSF) that contained (in mM): 1.25 NaH_2PO_4, 1.0 $MgCl_2$, 125.0 NaCl, 2.5 KCl, 2.0 $CaCl_2$, 25.0 $NaHCO_3$, and 10.0 glucose. Slices were incubated in oxygenated ACSF at 34°C for 30 min and kept at room temperature before being transferred to the recording chamber. Animal experiments were performed according to methods approved by the Animal Experimentation Ethics Committee of the Australian National University, Australia.

2.4 Fluorescence imaging of neurons

Pyramidal cells in layer V in the somatosensory cortex were chosen as target neurons in the slices. The neuron was patched with a glass electrode (resistance: 4–6 MΩ) containing (in mM): 115.0 K-gluconate, 20.0 KCl, 10.0 HEPES, 10.0 phosphocreatine, 4.0 ATP-Mg, 0.3 GTP, 5.4 biocytin, and 300 μM of AlexaFluor-488 (Sigma-Aldrich). The dye was allowed to diffuse into the neuron for 20–30 min before imaging. Image stacks with pixel dimensions of 500 X 500 pixels were obtained with 1-μm increments in the *z*-direction. *ImageJ* was used for 3D visualization of the cell. Image acquisition triggers the temporal gating of the incident laser via the AOM. Neurons at different depths in the slice were selected and imaged using the same procedure except that images were taken at only one plane for these experiments.

2.5 Electrophysiology

The neurons were tested for their viability and functionality by recording the membrane's voltage response and action potentials in response to a depolarizing current pulse in current clamp mode. Photodamage of the neurons was quantified by recording the current across the cell membrane before and after obtaining the image. The glass electrode used to fill the cell with dye was also used as the recording electrode. Recording of input membrane currents was done in whole-cell voltage clamp mode using a MultiClamp 700B amplifier (Molecular Devices). Action potentials from the cells were recorded in whole-cell current clamp mode using the same amplifier. Only cells with a stable resting membrane potential from the start of the patch were chosen for recording. The input resistance (R_{in}) of a cell was extracted from the voltage response to the application of small current steps (500 ms duration, steps in increments of 40 pA, 1 Hz) through the recording electrode, and extracting the slope value. The values of R_{in} across cells in the brain slices varied between 10 MΩ to 100 MΩ. R_{in} was obtained for each cell both before and after imaging, and analysis was done using *Axograph X* (Axograph Scientific). The error in the value of R_{in} was obtained from the standard deviation in the voltage traces. The results were accepted only for mean differences in R_{in} with significance in Student' t-test (P_t) <0.001.

#247308 Received 6 Aug 2015; revised 11 Sep 2015; accepted 11 Sep 2015; published 17 Sep 2015

3. Results and discussion

3.1 Imaging neurons using temporal gating

We utilized the temporal gating setup to image neurons in brain tissue and compared it with imaging in un-gated mode. We observed that temporal gating could be utilized to efficiently image a neuron at very low average powers as compared to imaging without temporal gating. Figure 3 shows images of layer V cortical pyramidal neuron obtained with and without temporal gating of the imaging laser at low values of $\langle P_{out} \rangle$ = 0.5 mW. Figure 3(a) shows a weak image of the neuron obtained without temporal gating. With temporal gating (Figs. 3(b)-3(d)) and maintaining $\langle P_{out} \rangle$ = 0.5 mW for various gating frequencies, the neuron's soma and dendrites appear visible. Highest fluorescence signal is achieved when the gating frequency is set to 0.4 MHz.

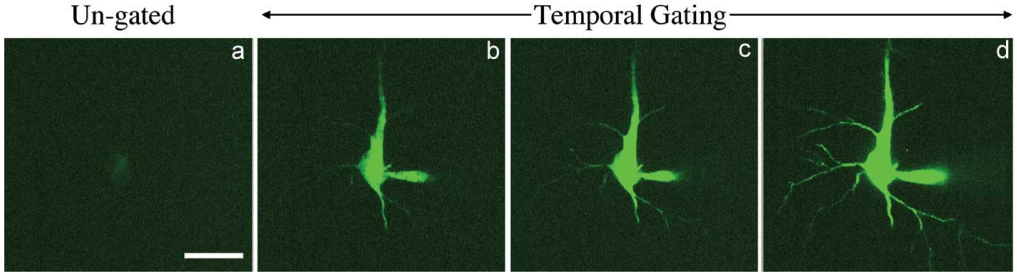

Fig. 3. Images of a layer V cortical pyramidal neuron obtained (a) without and with temporal gating with frequencies set at: (b) 2.4 MHz; (c) 1.2 MHz and (d) 0.4 MHz. All the images were taken at $\langle P_{out} \rangle$ = 0.5 mW. Scale bar = 20 μm.

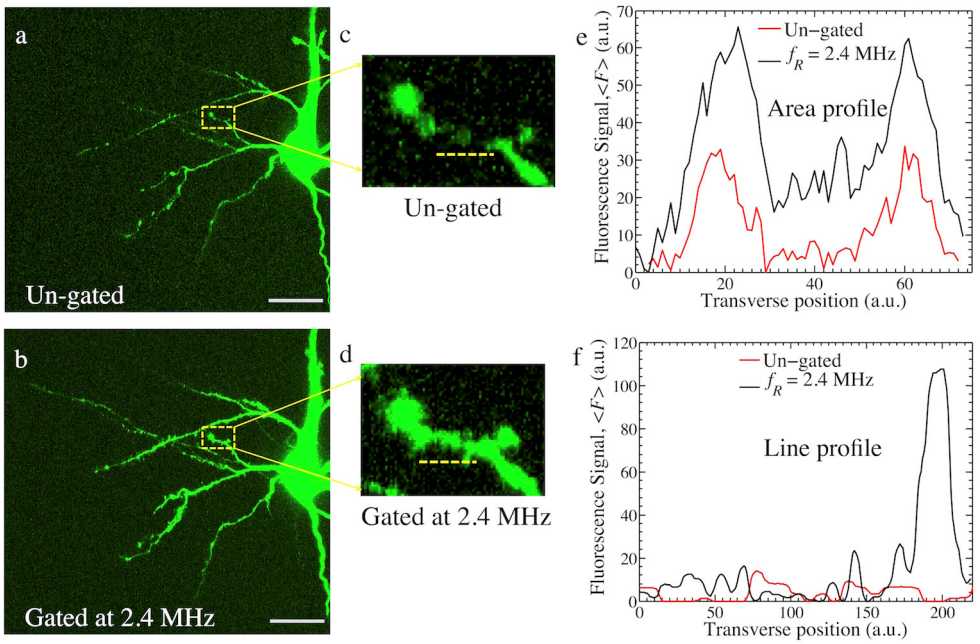

Fig. 4. Projected 3-D images of active neurons in a brain slice, imaged (a) without temporal gating (b) at 2.4 MHz gating frequency, for a constant $\langle P_{out} \rangle$ = 2.5 mW. Scale bar = 20 μm. Panels (c), (d) show a selected dendritic area from the neuron for the two modes in (a) and (b) respectively. Panel (e) compares the relative fluorescence intensity profiles measured for the selected areas in (a) and (b), and panel (d) shows the fluorescence profiles along the highlighted line in (c) and (d) respectively.

#247308 Received 6 Aug 2015; revised 11 Sep 2015; accepted 11 Sep 2015; published 17 Sep 2015

Figures 4(a) and 4(b) show the 2P images of a neuron in a brain slice as obtained without temporal gating and at a gating frequency of 2.4 MHz. Both sets of data were collected for a higher average power, $<P_{out}>$ = 2.5 mW. A comparison between Figs. 4(a) and 4(b) show that the image obtained using temporal gating is brighter. This image is also sharper, and some of the finer dendritic structures like spines are visible. A magnified area in the two images is also compared in the figure. The respective profiles of fluorescence intensities as a function of position over these images are shown in Figs. 4(c) and 4(d). The peaks in these images correspond to the features of the neuron body, and as observed in Fig. 4(d), the dendritic structures (spines) have higher intensity peaks and hence are significantly clearer. The enhancement in fluorescence emission from neuronal structures with temporal gating in the frequency range ~2.4 MHz is up to five-fold when compared to the un-gated mode for imaging.

These results were consistent for cells within a brain slice, as well in slices from different animals. The results show that temporally gating the laser results in improved fluorescence emission from the neuron in a brain slice. In two-photon imaging, the option of increasing the laser power to obtain higher fluorescence is usually limited by the possibility of photodamage to the cells and hence, maintaining a low powers to obtain higher fluorescence is usually desirable. The temporal gating technique shown here simultaneously maintains a low photon flux and enhances the fluorescence emission from the sample when compared to imaging without temporal gating. It hence offers a superior way to improve fluorescence imaging of biological samples.

We further investigated if the temporal gating technique could be utilized to image cells located deep within the brain slice. Neurons at various depths in the brain slices were selected and imaged at various gating frequencies. The relation between fluorescence as a function of the depth of the neurons' soma in the slice for various gating frequencies is shown in Fig. 5. As expected, the fluorescence from a cell decreases as a function of its depth in the tissue due to scattering. However, it can be seen from the plots that temporal gating improves the fluorescence signal at all depths, and gated excitation of a neuron deep in the tissue yields a significantly higher signal compared to the constant excitation.

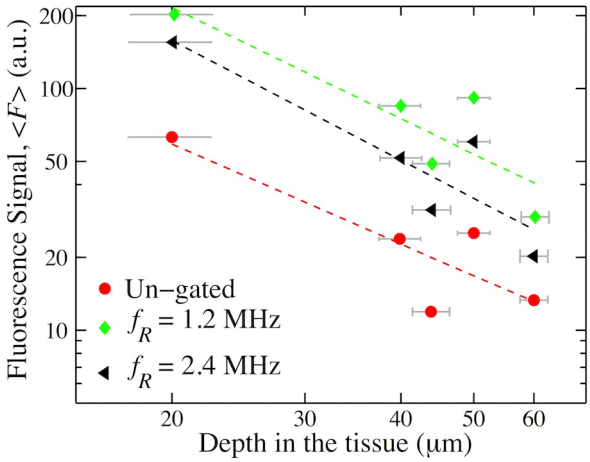

Fig. 5. Fluorescence intensity measured as a function of depth of the neurons within the brain tissue, shown for 1.2 MHz and 2.4 MHz frequencies, and compared with those obtained without gating. The data corresponding to each depth on the x-axis is from the same cell.

Acquiring images through significant depths of physiological systems such as the brain has been a challenge because the heterogeneity results in strong scattering by the various tissue components, and limits the spatial resolution necessary to resolve individual neurons

#247308 Received 6 Aug 2015; revised 11 Sep 2015; accepted 11 Sep 2015; published 17 Sep 2015

and neuronal processes. Although recent work with 2P imaging techniques have enabled the imaging of neurons up to 1.6 mm deep inside a mouse brain *in vivo* [35], it has been difficult to penetrate deeper than that. Our results show that temporal gating of laser pulses in the range 1-3 MHz offers the ability to achieve a higher fluorescence signal from living cells deeper in the tissue and is hence a promising tool that could be integrated with/incorporated into existing techniques for deep brain imaging and optogenetics.

3.2 Implications for photodamage

As discussed in the sections above, the idea of temporal gating enables one to image fluorescence from a neuron at reduced average power of the 2P laser. The reduced values of average powers point to a lower probability of photodamage caused by the laser beam to the cells. We carried out a set of experiments to quantify the photodamage of the neuronal cells whilst using the temporal gating method for imaging. In these experiments, the selected neuron in the physiologically maintained brain slice was filled with the dye solution for imaging, tested for its viability and functionality, and the membrane input resistance, R_{in} was recorded before and after imaging with the 2P technique, with and without temporal gating. Also, the $<P_{out}>$ was adjusted in a range to maintain a pre-set maximum fluorescence signal in the images acquired at the different gating frequencies.

We expected that the occurrence of photodamage during the 2P imaging would cause a change in cell membrane's ion permeability, thereby resulting in a change in the value of R_{in} after the imaging. We therefore take the magnitude of change in the membrane's input resistance (ΔR_{in}) as the measure of photodamage. Typical results from a neuronal cell are presented in Fig. 6. It appears that the change in the input resistance, where $|\Delta R_{in}| = |R_{in(\text{before imaging})} - R_{in(\text{after imaging})}|$ follows a certain trend across the gating frequencies. The ΔR_{in} is minimum at 2.4 kHz, and then starts to increase as the temporal gating frequency is reduced to 0.4 MHz, and is also higher for the un-gated mode of imaging. This trend was consistent across neurons within or in different brain slices. Our results imply that ~1.2 - 2.4 MHz is an optimum gating frequency range at which photodamage of the cell membrane is minimal.

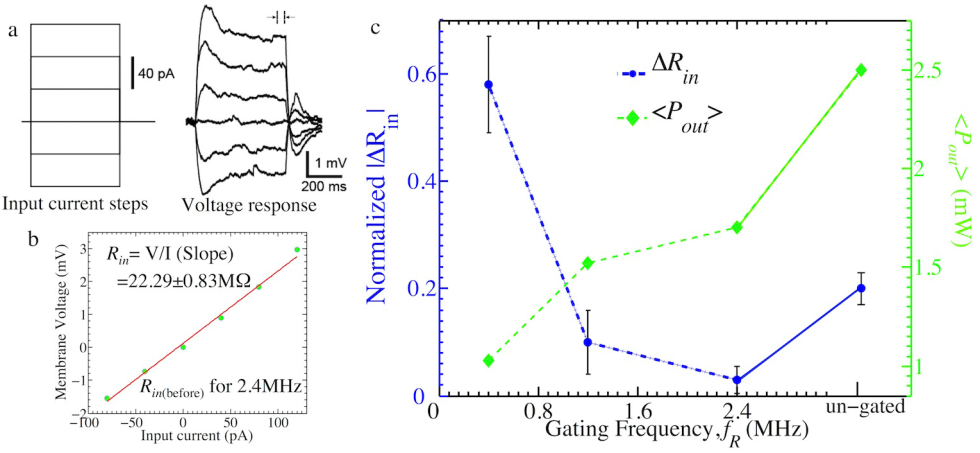

Fig. 6. (a) Representative profile of membrane voltage across a neuronal cell in response to input current steps. The membrane voltage value is calculated at the arrows marked. (b) An example of the membrane-voltage-current response curve from which R_{in} values are calculated. (c) A typical behavior of change in a cell's input resistance (ΔR_{in}) as a function of gating frequency, f_R and corresponding $<P_{out}>$. Here, Normalized $|\Delta R_{in}| = |R_{in(\text{before imaging})} - R_{in(\text{after imaging})}|/R_{in(\text{before imaging})}$. The error bars in $|\Delta R_{in}|$ are calculated from the standard deviation of membrane voltage in panel (a). Solid lines have been used to show discontinuity between gated and un-gated modes of imaging.

#247308 Received 6 Aug 2015; revised 11 Sep 2015; accepted 11 Sep 2015; published 17 Sep 2015

It is possible that imaging with a temporally gated 2P laser with a high bunch-pulse energy results in a non-linear interaction with the cell membrane, causing more photodamage compared to prolonged exposure to a low power un-gated laser. However, quantification of this dependence has not been carried out in this study. Further, a limitation set by our existing instrumentation is the pulse-width of the temporal gate. We are currently limited to the speed of the DAQ, which sets a minimum bunch-pulse width of σ = 140 ns. The relatively long bunch-pulse width could have possibly affected the neurons at the lowest repetition rate (0.4 MHz) equivalent to one gated bunch per pixel. However, with the current device limitation, it is difficult to decrease the bunch-pulse width and show its effect. Furthermore, the gating frequency f_R = 2.4 MHz is another limitation of our instrumentation. It should also be noted that in the experiments for quantification of photodamage, the pre-set maximum fluorescence signal was kept in a low range where the photodamage could be observed within one cell for all gating frequencies, but was not drastic enough to damage the cell after imaging at one frequency. This could also be one of the reasons of low magnitudes of ΔR_{in} observed in our studies (the magnitude for change in R_{in} varied in the range 0.1 - 15 MΩ).

High peak powers to enhance fluorescence have been previously used in saturated excitation imaging of various materials including biological cells [36–38]. However, these studies have focused on achieving high spatial resolution. It has also been shown previously that having one femtosecond pulse per pixel, like the implementation with regenerative amplifiers [30], could improve the fluorescence yield from samples. However, there has been no study yet of using regenerative amplification of laser pulses and its effect on cellular membranes similar to what have been provided in this work. Regenerative amplifiers operate on a pre-set wavelength and designed with slow repetition rates (10 to 250 kHz) that could limit the speed of image acquisition. Nevertheless, combining the regenerative amplification with a passive pulse splitting optical setup [28] could be used to increase the repetition rates of regenerative amplifiers as integral multiples of the base frequency, which could in turn be used to achieve high fluorescence yield whilst reducing photodamage. Our temporal gating technique attains improved fluorescence signal whilst inflicting low photodamage on living cells and therefore presents a far simple and cost-effective way to achieve improvement that approaches a system, which uses a regenerative amplifier.

4. Conclusion

In this work, we have improved 2P imaging of living neurons in brain tissue by temporal gating of the incident femtosecond-pulse laser. The set-up of temporal gating was integrated with a 2P laser scanning microscope to image neuronal cells in brain slices and obtain enhanced fluorescence from the deeper layers of the tissue. While using this technique, we could further maintain minimal average laser power incident on the sample, thereby overcoming the limitations of photodamage of the sample and photobleaching of the fluorophores. In addition to fluorophore stability, we report an optimal range of gating frequency, which maintains cell viability whilst improving fluorescence yield. In this frequency range, the photodamage to the cells is minimal, yet the fluorescence emission is up to five-fold higher than that obtained with un-gated mode of imaging. Our work highlights the use of temporal gating for imaging fluorescence from living biological samples where cell viability and photodamage are issues of major concern. Ongoing studies are directed towards integrating the temporal gating technique with our existing 2P microscope [10,11] for multi-site photochemical stimulation of neurons.

Acknowledgment

This work was supported by the Australian Research Council Discovery Project (contract number DP140101555).

#247308 Received 6 Aug 2015; revised 11 Sep 2015; accepted 11 Sep 2015; published 17 Sep 2015